ChemComm
Chemical Communications

Accepted Manuscript

This article can be cited before page numbers have been issued, to do this please use: E. J. Evans and L. Clark, *Chem. Commun.*, 2026, DOI: 10.1039/D6CC02624A.

ROYAL SOCIETY OF CHEMISTRY

rsc.li/chemcomm

View Article Online
DOI: 10.1039/D6CC02624A

Journal Name

ARTICLE TYPE

Cite this: DOI: 00.0000/xxxxxxxxxx

Developing Scotch tape Exfoliation Methods for Two-Dimensional Magnetic Metal-Organic Frameworks

Elizabeth J. Evans[a] and Lucy Clark[a*]

Received Date
Accepted Date

DOI: 00.0000/xxxxxxxxxx

The emergence of two-dimensional materials has transformed solid-state chemistry and condensed matter physics, yet intrinsic magnetism remains rare in atomically thin systems. Magnetic metal–organic frameworks (MOFs) offer a compelling and chemically versatile platform to address this challenge, combining tuneable magnetic interactions with crystal structures amenable to exfoliation. In this Review, we examine the development of the micro-mechanical "Scotch tape" method for the isolation of two-dimensional magnetic MOFs, benchmarking it against established exfoliation approaches and highlighting its unique ability to yield larger, higher-quality nanosheets. Through key case studies, we assess the current state of the field, identifying critical limitations including poor reproducibility, insufficient methodological reporting, challenges in crystal growth, and difficulties in applying surface-sensitive magnetic characterisation techniques. We further discuss how these barriers may be overcome through community-driven standardisation of exfoliation protocols, advances in crystal engineering, and the integration of computational and data-driven approaches to predict exfoliation behaviour. Finally, we outline emerging opportunities for tailoring magnetic and surface properties in MOF nanosheets, positioning Scotch tape exfoliation as a powerful yet underutilised route toward the rational design and discovery of next-generation two-dimensional magnetic materials.

Introduction

The isolation of graphene in 2004, through mechanical "Scotch tape" exfoliation, marked a turning point in materials research, giving rise to the modern field of two-dimensional materials.[1] This ostensibly simple method has since been broadly applied to a range of layered inorganic solids, most prominently transition metal dichalcogenides (TMDs),[2 3 4] hexagonal boron nitride (hBN),[5] and layered perovskite materials,[6–8] enabling systematic exploration of atomically thin crystals.[9] Although these exfoliated two-dimensional inorganic materials display an exceptional array of electronic, optical, and mechanical properties,[10–16] intrinsic magnetism is relatively uncommon among them.[17] The development of atomically thin magnetic systems is, therefore, of considerable interest. From a fundamental standpoint, such materials provide a platform to probe long-standing theoretical concepts, most notably the role of magnetic anisotropy in stabilising long-range magnetic order in two dimensions in light of the Mermin–Wagner theorem,[18] and to investigate spin interactions, phase transitions, and quantum phenomena in the monolayer limit.[19,20] From a technological perspective, two-dimensional magnets also present opportunities for next-generation devices, particularly in spintronics and information storage, where their potential for electrical or optical control, and compatibility with van der Waals heterostructures, could enable ultra-thin, low-power magnetic technologies.[21–24]

Thus, another major breakthrough in the field was the application of the Scotch tape method for the exfoliation of magnetic CrI_3 and $Cr_2Ge_2Te_6$, yielding monolayer and bilayer samples in each case, respectively, and the demonstration of their intrinsic ferromagnetism in the two-dimensional limit.[25,26] These systems represent the first experimental realisations of two-dimensional ferromagnetism, discoveries which came almost fifty years after their theoretical prediction in the 1970s.[27] Indeed, these discoveries paved the way for subsequent realisations of long-range magnetic order in monolayers of other inorganic systems, Fe_3GeTe_2, VSe_2, $FePS_3$ and $NiPS_3$.[28–31] However, in terms of their characterisation and eventual translation into devices, these inorganic materials present several challenges, including their chemical instability in the two-dimensional limit[32–38] and their limited chemical tunability.[39]

In this regard, an attractive alternative class of materials which has since emerged are magnetic metal-organic frameworks (MOFs).[40] MOFs are composed of metal nodes connected by organic linkers into extended three-dimensional crystalline struc-

[a] School of Chemistry, Molecular Sciences Building, University of Birmingham, Edgbaston, Birmingham, B15 2TT, UK. E-mail: l.m.clark@bham.ac.uk

View Article Online
DOI: 10.1039/D6CC02624A

tures that are particularly well-suited for reticular materials design strategies.[41] Indeed, the chemical tunability of MOFs enables many potential applications[42–45] that are widely celebrated, most recently through the 2025 Nobel Prize in Chemistry.[46] *Magnetic* MOFs are particularly attractive because their paramagnetic metal ions and organic linkers can be readily exchanged to tailor their magnetic anisotropies and exchange interactions.[47,48] For instance, layered magnetic MOFs are made up of paramagnetic metal nodes connected by organic linkers into extended two-dimensional planes, which are layered in the third dimension by weak intermolecular forces.[49] The weak intermolecular forces between their two-dimensional layers makes such MOFs susceptible to exfoliation and thus, promising candidates for exploring, tuning and exploiting magnetism in materials which are stable in the two-dimensional limit.[50–52] To date, the exfoliation of MOFs into two-dimensional structures has largely been achieved by ultrasonic or chemical exfoliation techniques. Despite its widespread use in the exfoliation of inorganic materials and graphene, the application of the Scotch tape method to layered MOFs has only been reported in a handful of cases. In this review, we highlight the recent advances in the development and application of the Scotch tape method for layered MOFs. In particular, we focus on the development of this methodology for the realisation of new, chemically versatile two-dimensional magnetic MOFs and present what we propose to be the greatest challenges in adapting the Scotch tape method for MOFs and how we may overcome these limitations.

Current exfoliation techniques for layered MOFs

The first exfoliation of a layered MOF was reported in 2008, when $Zn(C_{12}H_{14}O_4)$ layers were successfully exfoliated into monolayers using solvent-mediated ultrasonic exfoliation.[53] Since then, this method has become the most widely employed strategy for MOF exfoliation, in which solvent choice and ultrasonic frequency, along with sonication temperature and time, are typically adjusted for material-specific requirements.[49] This technique can be applied to a wide variety of layered MOFs, and even to polycrystalline samples,[53] which is useful considering that the single-crystal growth of MOFs can be challenging to reproduce.[54] Tyndall scattering and dynamic light scattering (DLS) are typically employed to confirm the presence of MOF nanosheets in solution,[55] and deposition onto flat substrates by, for example, drop casting, allows atomic force microscopy (AFM) to be used to characterise nanosheet height and lateral size.[56] Whilst this technique often successfully yields ultra-thin (monolayer thickness) nanosheets, they are typically only a few hundred nanometres in width and substrate coverage can be poor.[57] This precludes most surface-sensitive chemical, structural and physical property characterisation techniques, limiting further investigation of nanosheet properties and creating ambiguity over whether chemical composition and crystallinity have been retained upon exfoliation.

Other exfoliation methods applied to MOFs include chemical exfoliation, which typically involves synthesis of a three-dimensional structure with interlayer ligands that can be chemically cleaved. This has most notably been explored in a MOF with disulfide bridging ligands which can be selectively cleaved to produce ultra-thin nanosheets up to 10 μm wide.[58] This technique, however, requires specific conditions for selective bond cleavage. In addition, the preferred conformation of the disulfide bond in common dipyridyl bridging ligands[59] may disturb the desired topology within the two-dimensional layers of interest. As such, new, alternative methods of targeted chemical cleavage for MOF exfoliation are also being explored. For example, researchers at the Catalan Institute of Nanoscience and Nanotechnology have developed a novel de-reticulation strategy, which they term 'Clip-off Chemistry'.[60] This has been successfully applied to a three-dimensional Zr-polycarboxylate MOF, where programmed interlayer bond cleavage with high specificity yields a layered MOF which can then be exfoliated into two-dimensional sheets.[61] Bottom-up methods, such as chemical vapour deposition (CVD) or molecular beam epitaxy (MBE), have been shown to produce large MOF monolayers, making surface-sensitive characterisation more facile, but these techniques often require higher temperatures and extreme conditions, which most MOFs and their precursors cannot tolerate.[62,63]

The final general class of exfoliation used for MOFs is mechanical exfoliation. This encompasses methods like ball-milling and grinding,[64] as well as the micro-mechanical "Scotch tape method."[1] Scotch tape exfoliation, the technique initially used to afford single-layer graphene, involves the use of adhesive tape to pull apart weakly-bound layers and deposit them on flat substrates (Fig. 1). This is arguably the most popular exfoliation technique for layered materials in general, having been widely applied to many inorganic layered materials, yet its application to layered MOFs is surprisingly limited. In cases where it has been used,[50–52,65–68] MOF nanosheets of lateral sizes up to 10 μm have been obtained, even down to the single layer in some cases. Substrate coverage of exfoliated material after deposition is typically better than for chemical and ultrasonic methods,[65] and the larger nanosheets obtained allow for easier confirmation of the resulting crystallinity and chemical composition of the exfoliated material. Despite this promise, there remain several limitations for the application the Scotch tape method to the exfoliation of MOFs, which we highlight in the following sections. We argue that these challenges need to be addressed and fully reported in order for the full potential of this methodology to be realised within the MOF community.

Recent advances in the Scotch tape exfoliation of layered MOFs

The first application of Scotch tape exfoliation to a layered MOF was reported in 2015.[65] In this report by Abhervé *et al.*, a family of magnetic layered MOFs, with general formula $[M^{3+}(L_2\text{-trien})][Mn^{2+}Cr^{3+}(X_2An)_3]$ (M = Fe or Ga, L = acetylacetonate (acac) ligand or salen (sal) ligand and X = Cl or Br) were successfully synthesised. These MOFs were then exfoliated both by Scotch tape and ultrasonic exfoliation methods, where the former produced larger, more crystalline nanosheets than the

View Article Online
DOI: 10.1039/D6CC02624A

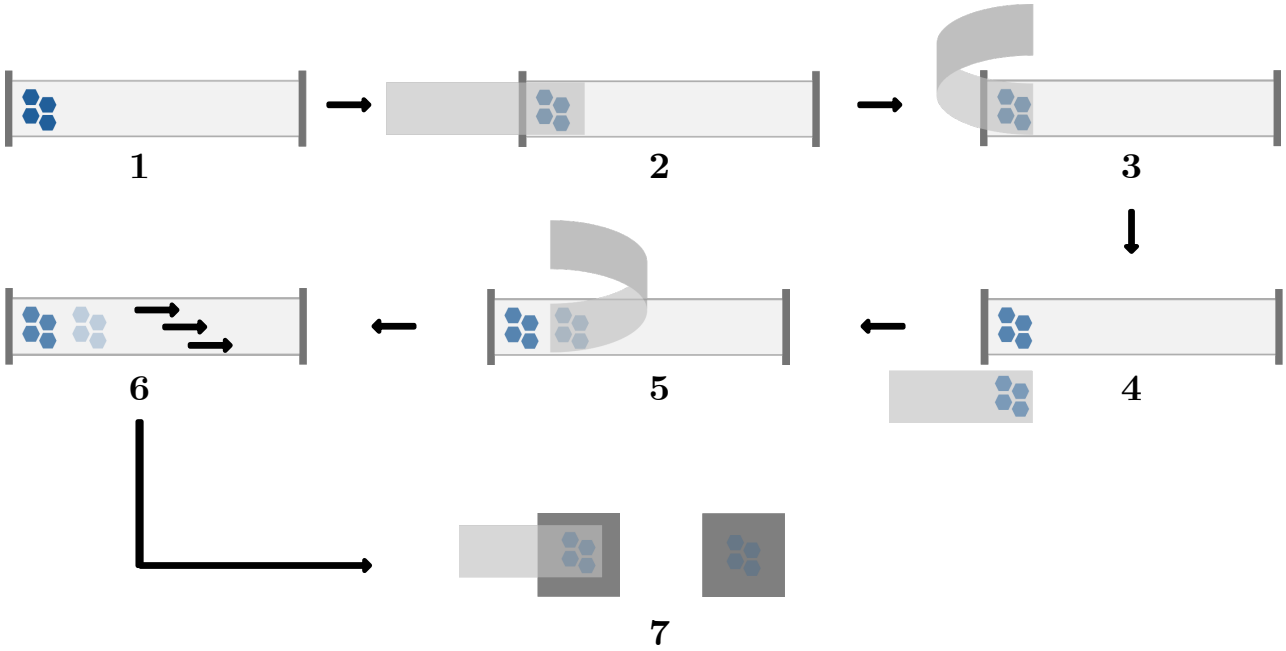

Fig. 1 Schematic showing the general "Scotch tape method", as first developed by Novoselov *et. al.* to intially obtain single-layer graphene.[1] 1. Single crystals of the layered material are stuck flat to a piece of adhesive tape. 2. Another piece of tape is gently pressed on top of the crystals. 3. The tape is peeled away, leaving exfoliated material on both pieces of tape. 4. The tape that has been peeled away is then gently stuck back down on the first piece of tape. 5. It is then peeled away again, yielding thinner exfoliated material on both pieces of tape. 6. This process is repeated as many times as is desired. 7. Exfoliated nanosheets are deposited onto a flat substrate, typically Si/SiO_2.

latter. Two of the MOFs reported in this study consist of anionic honeycomb layers in the *ab*-plane, where Mn^{2+} $S = 5/2$ and Cr^{3+} $S = 3/2$ ions occupy alternating vertices of the hexagons within the honeycomb layers, and are linked by halide-functionalised anilate bridges (X_2An, X = Cl or Br) as can be seen in Fig. 2. $[Fe^{3+}(acac_2\text{-trien})]^+$ cationic complexes sit within the hexagonal channels to charge balance the framework, forming an overall charge-neutral layered MOF, where the anilate layers stack in the *c*-direction and are held together by weak van der Waals forces between the Cl or Br atoms. The third MOF reported in this study has the same in-plane structure (X = Br), but instead possesses a diamagnetic Ga^{3+} cationic complex in the central channel in place of $[Fe^{3+}(acac_2\text{-trien})]^+$.[65] The fourth incorporates a different chelating ligand for the Fe^{3+} cation, $[Fe^{3+}(sal_2\text{-trien})]^+$, which results in a structure with alternating anionic/cationic layers held together by electrostatic interlayer interactions.[69] In each case, for bulk samples, there is an antiferromagnetic arrangement of $S = 3/2$ Cr^{3+} and $S = 5/2$ Mn^{2+} ions, leading to long-range ferrimagnetic order below their respective ordering temperatures, T_N = 10.4 K, 11.8 K, 11.6 K, 10.0 K. In addition, there is a paramagnetic contribution from the Fe^{3+} ions in the cationic complexes, which remain in the high-spin state ($S = 5/2$).[65]

Due to the weak van der Waals forces between the layers in these MOFs, exfoliation techniques can be used to separate them. Single crystals were grown via a solvothermal synthesis method, and scanning electron microscopy (SEM) images reveal a layered morphology. Scotch tape exfoliation successfully yielded flakes varying in lateral size and thickness, with a reported random distribution across the Si/SiO_2 substrate on which they were deposited.[65] The atomic force microscopy (AFM) images presented in the main manuscript and supplementary information of Ref. 65 show that the largest flakes measure up to 5 μm in diameter, with thicknesses between $10-20$ nm, corresponding to $\sim 10-20$ layers, where a single layer is approximately 0.7 nm in height. Smaller flakes of up to 800 nm in diameter and as thin as 2 nm (*i.e.* approaching bilayer height) were also obtained.[65] Abhervé *et al.* also showed that the electrostatic MOF can be exfoliated using Scotch tape exfoliation, yielding nanosheets as large as 20 μm in diameter (with thickness $\sim$ 60 nm) and as thin as 2 nm (with up to 300 nm lateral width), corresponding to a single cation/anion hybrid layer.[69] For comparison, two of the MOFs were also exfoliated using ultrasonication. In general, for both MOFs, flakes were smaller laterally (up to a few hundred nm) and thicker (the thinnest $\sim$ 5 nm) when obtained by ultrasonication in comparison to the Scotch tape method. It is also evident from the AFM images in Ref. 69 that the nanosheets obtained by ultrasonication have more poorly defined edges, possibly indicating that they are less crystalline than the large, angular nanosheets obtained by the Scotch tape method (Fig. 3).

This milestone study clearly illustrates that Scotch tape exfoliation can be applied successfully to layered MOFs, and demonstrates that it even out-performs the more popular ultrasonication exfoliation technique, delivering thinner, larger, better-quality nanosheets. Yet, we argue that the report lacks a sufficiently detailed methodological description of the Scotch tape exfoliation procedure used to obtain the nanosheets, and does not provide any statistical analysis or indication of the

View Article Online
DOI: 10.1039/D6CC02624A

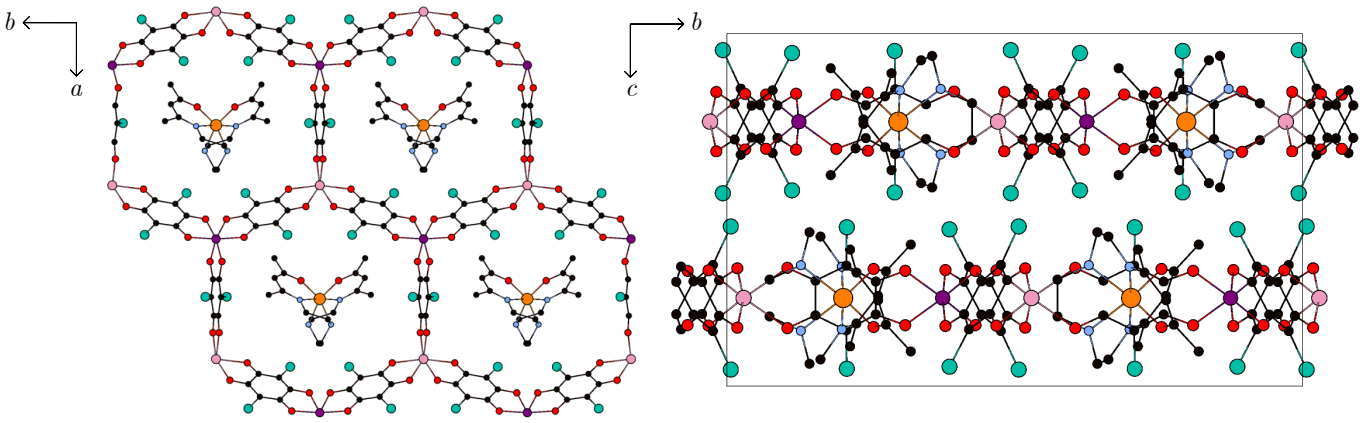

Fig. 2 (*Left*) A single layer of $[Fe^{3+}(acac_2\text{-trien})][Mn^{2+}Cr^{3+}(Br_2An)_3]$ shown in the *ab*-plane. Alternating Cr^{3+} and Mn^{2+} ions are bridged by anilate ligands, forming a honeycomb structure. Charge-balancing $[Fe^{3+}(acac_2\text{-trien})]$ cations sit in the hexagonal channel of the MOF. (*Right*) Two adjacent layers, stacked in the *c*-direction, are shown. Van der Waals interactions between the bromine atoms on the functionalised anilate ligands hold the layers together. Mn, pink; Cr, purple; Fe, orange; C, black; N, light blue; O, red; Br, teal. Hydrogen atoms and solvent molecules have been omitted for clarity.

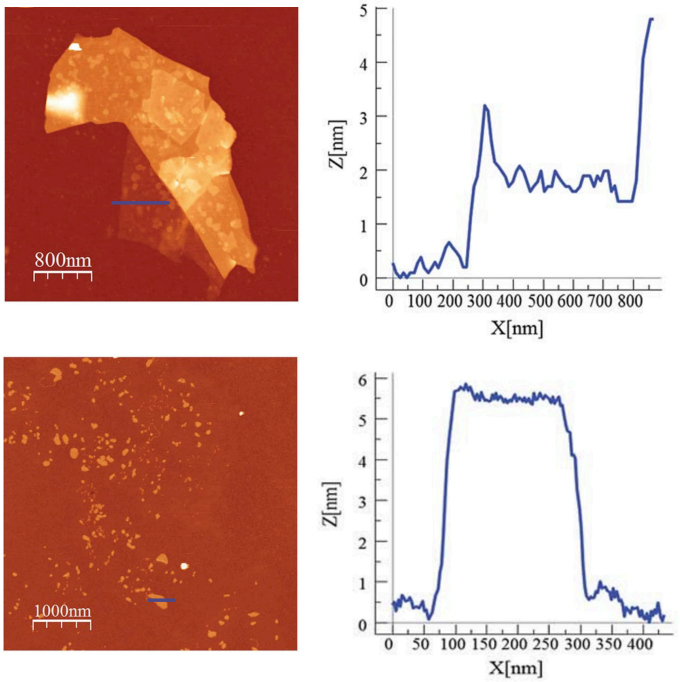

Fig. 3 (*Top, left*) AFM topographical image showing a nanosheet of $[Fe^{3+}(acac_2\text{-trien})][Mn^{2+}Cr^{3+}(Br_2An)_3]$ obtained *via* Scotch tape exfoliation. The blue line corresponds to the line profile (*top, right*), which indicates the section of flake has a height of $\sim$ 2 nm, corresponding to the bilayer height. (*Bottom, left*) AFM topographical image showing nanosheets of $[Fe^{3+}(acac_2\text{-trien})][Mn^{2+}Cr^{3+}(Br_2An)_3]$ obtained *via* ultrasonic exfoliation of single crystals in ethanol. The blue line corresponds to the line profile (*bottom, right*), which indicates an average nanosheet of lateral width $\sim$ 250 nm μm and height $\sim$ 5 nm ($\sim$ 5 layers). Here we can clearly see that nanosheets obtained *via* Scotch tape exfoliation are typically much larger laterally, and have angular, well-defined edges. In comparison, nanosheets obtained *via* ultrasonic exfoliation are much smaller and edges are less well-defined, possibly indicating poorer crystallinity. Figures adapted from Ref. 65 with permission from the Royal Society of Chemistry,[65] copyright 2015.

reproducibility of the exfoliation methods used. There are also a number of artefacts in the AFM images presented, which may indicate challenges with substrate cleanliness and/or adhesive contamination,[70] but these are not explained. This can lead to difficulty in interpreting the results presented as a reader, as it is challenging to distinguish what is sample from possible contamination in microscopy imaging. We propose, however, that this is not uncommon, as limitations in the reporting of Scotch tape exfoliation methods have been perpetuated from its very first use.[1] For a technique so widely-used in the two-dimensional materials community, detailed method statements are often lacking throughout the scientific literature. Instead, this appears a technique in which expertise is more commonly passed through groups anecdotally, making it less accessible to the wider scientific community. We suggest that this may be one of the key barriers to its wider adoption by the MOF community, where additional challenges, such as weak inter-plane interactions, small crystal sizes and increased crystal fragility, make a nuanced, detailed understanding of the technique all the more critical.

Another important case study in the Scotch tape exfoliation of layered MOFs is the 2018 paper from López-Cabrelles *et al.*.[50] In this study, the authors prepare a series of MOFs in the MUV-1-*X*(Fe) family, with the general formula $[Fe(bimX)_2]$, where bim*X* is the benzimidazole ligand functionalised at the 5-position with X = H, Cl, Br, CH_3, NH_2,[50] or F.[52] Here, the pre-synthetic ligand functionalisation, made possible by the versatility of chemical space offered by MOFs, yields layered MOF crystals which are proposed to retain their crystallinity upon exfoliation down to the few-layer and monolayer limit.[50] Within the crystal structure, distorted tetrahedral Fe^{2+} $S = 2$ ions are connected by Hbim*X* ligands to form neutral layers in the *ab*-plane. These layers are then held together by weak van der Waals forces between the *X* substituents in the layers (Fig. 4) Below their respective Néel temperatures in bulk, $T_N \approx 20$ K, the MUV-1-*X*(Fe) family adopt a canted antiferromagnetic ground

View Article Online
DOI: 10.1039/D6CC02624A

state, as confirmed by d.c. and a.c. susceptibility magnetometry studies on bulk powder MOF samples.[50]

In this study of López-Cabrelles *et al.*, the use of "Ultron Systems" plastic tape is reported for the exfoliation, which, anecdotally, is preferred within the two-dimensional materials community because it typically leaves less adhesive residue compared to the Scotch Magic^{TM} tape brand. However, it is also generally considered that this tape is less well-suited to materials that are more difficult to cleave, *i.e.*, those with stronger inter-plane interactions, since there is less adhesive on the tape overall. Nanosheets were deposited on Si/SiO_2 substrates, and the exfoliation provided good coverage of nanosheets with typical lateral dimensions greater than 1 μm, and varying thicknesses from 1.5 nm (corresponding to the monolayer, Fig. 5) to hundreds of nm.[50] The authors confirm that both the structural and chemical composition of MUV-1-Cl(Fe) are retained on exfoliation through transmission electron microscopy (TEM) and Raman spectroscopy, respectively. They also perform low-temperature magnetic force microscopy (LT-MFM) measurements on exfoliated flakes to ascertain whether the magnetic behaviour seen in bulk is retained on exfoliation. Whilst they detect a small ferromagnetic signature, which may be associated with the canted antiferromagnetic ground state observed in bulk, one cannot unequivocally conclude that the observed signal is purely magnetic and does not have any contribution from electrostatic forces.[50]

This highlights another challenge for the field, which is that surface-sensitive magnetic characterisation of MOF nanosheets is particularly difficult. Techniques commonly applied to inorganic two-dimensional materials, like magneto-optic Kerr effect (MOKE) microscopy,[25,26] require large, uniform flakes, at least several microns in width. This is particularly difficult to achieve for MOFs, where metal-organic intra-plane bonds are typically weaker than in purely inorganic systems, leading to more fracturing of layers during exfoliation and, therefore, smaller lateral sizes of nanosheets compared to inorganic layered materials.[71,72] It is often observed, as in the case of Ref. 50, that Scotch tape exfoliation of MOFs also leads to substrate coverage by a variety of nanosheet thicknesses. In addition, it is also observed that a range of thicknesses exist within a single flake, as is illustrated by Fig. 5. This makes magnetic characterisation by techniques with large probe areas particularly difficult, because contribution from a variety of flake thicknesses can complicate measurements and analyses. This is particularly pertinent in the two-dimensional limit (monolayer, bilayer), where the emergent magnetic behaviour may be distinct from that observed in multiple layers and the bulk.[27,73]

López-Cabrelles *et al.* also investigated the surface behaviour of exfoliated flakes as a function of X substituents in MUV-1-X(Fe).[50] In particular, they investigated the hydrophobicity/hydrophilicity of exfoliated flakes through contact angle measurements of water droplets deposited on their surfaces. They observed that surface hydrophobicity changes with functional group X, showing that flakes with halide substituents (Cl, Br) show strong hydrophobic character, with alkane substituents (H, CH_3) showing moderate hydrophobic character and $X = NH_2$ showing super-hydrophilic behaviour. This highly tuneable surface behaviour highlights the advantages of MOFs over inorganic materials. It demonstrates how exploiting the reticular design principles inherent to MOFs might allow us to employ surface groups to make them more resistant to degradation in the two-dimensional limit.

One might imagine that changing X, which clearly affects the MOF surface energy, will also affect the inter-plane energies (*i.e.*, the strength of the van der Waals interactions between layers), and thus also affect the relative ease of exfoliation of each MOF, with those with stronger inter-plane energies being harder to exfoliate than those with weaker inter-plane interactions.[71] However, this comparison is not presented in Ref. 50. While it is stated that all members of the MUV-1-X(Fe) series presented can be exfoliated, only a single AFM image of flakes for each is shown in the supplementary information.[50] We suggest that the lack of such a comparison of exfoliation successes (and failures) within this family of MOFs presents an important opportunity for future studies. Comprehensive recording of the size of flakes, minimum thickness achieved, and the coverage and uniformity of flakes across multiple samples, coupled with appropriate statistical analysis would allow the "success" of exfoliation to be qualified and compared to other systems, which could in turn be rationalised by MOF structure and the magnitude of intra- and inter-plane interactions to guide future two-dimensional materials design.

In their subsequent 2021 study,[51] the same team investigated the effect of exchanging the Hbim$X$ ligand to bimX_2, where X = Cl or CH_3. This affords a change to the MOF structure, resulting in MUV-8-X(Fe). In this structure, the doubly-functionalised benzimidazole ligands cause the formation of an Fe^{2+}-based double-layer, where the tetrahedral Fe^{2+} $S = 2$ centres are connected by three ligands in the *ab*-plane and a fourth ligand connects to another Fe^{2+} in the *c*-direction (Fig. 6) These double layers are then held together by weak van der Waals forces between the X substituents on the ligand. In bulk, these compounds display canted antiferromagnetism below a $T_N \sim$ 23 K.[51] MUV-8-Cl(Fe) can also be successfully exfoliated *via* a Scotch tape method, yielding nanosheets as thin as 6 nm, which corresponds to $3-4$ layers. Raman spectroscopy of MUV-8-Cl flakes indicated that the chemical composition of the bulk is retained on exfoliation.[51]

In this paper, the authors also investigated the effect on the magnetic behaviour of the system of switching the metal ion in MUV-1-Cl(Fe) to Co^{2+} ($S = 3/2$) and Mn^{2+} ($S = 5/2$).[51] MUV-1-Cl(Co) still behaves as a canted antiferromagnet, but the Néel temperature, T_N, decreases to 11 K. In MUV-1-Cl(Mn), below $T_N = 14$ K, the system is antiferromagnetic without spin canting, confirmed by d.c. and a.c. susceptibility measurements, likely a result of the spin isotropy of d^5 Mn^{2+}. No comment is made

View Article Online
DOI: 10.1039/D6CC02624A

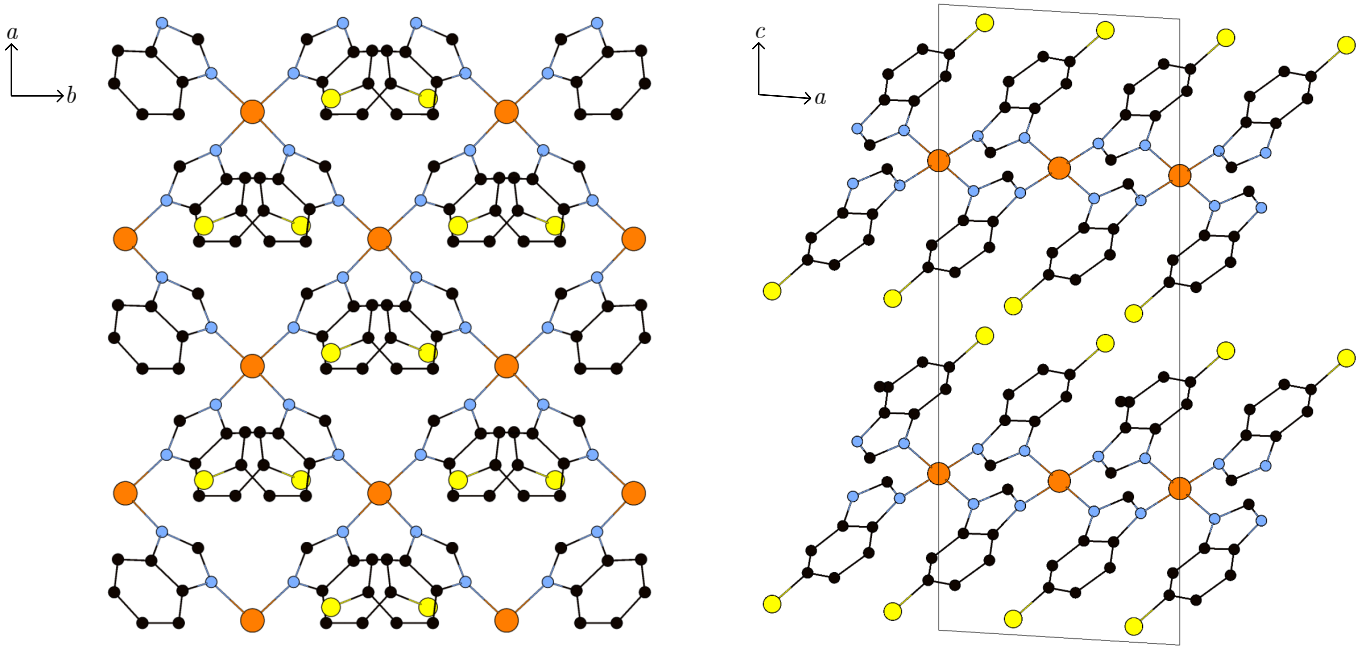

Fig. 4 (*Left*) A single layer of MUV-1-Cl(Fe) shown in the *ab*-plane. Tetrahedral Fe^{2+} centres are bridged by HbimCl ligands forming a square lattice. (*Right*) Two adjacent layers of MUV-1-Cl(Fe) shown stacked in the *c*-axis direction. Van der Waals interactions between the Cl atoms hold the layers together. Fe, orange; C, black, N, light blue; Cl, yellow. Hydrogen atoms, ligand disorder, and solvent molecules have been omitted for omitted for clarity.

on the effect of changing ligand, or metal ion, on the exfoliation of the MOFs, despite a significant change to the structure (Fig. 6), in the former case, and the bulk crystal morphology,[51] in the latter, both of which might be predicted to have an effect. However, in this study, the T_N of exfoliated flakes are extracted through nanomechanical resonance. Here, flakes are suspended over small circular cavities ($d = 5 - 6$ μm) and probed between $T = 4 - 50$ K using laser interferometry. The relationship between resonance frequency of exfoliated flakes and their specific heat is exploited to extract the transition temperature in each case.[74] In this way, it is shown that the T_N values of exfoliated flakes closely agree with the corresponding values for the bulk samples. Whilst this technique has been shown to work well for the family of insulating two-dimensional materials, MPS_3 (M = Fe, Ni, Mn),[74] it may be less widely applicable to MOFs. In this case, flakes of MUV-1-H(Co), MUV-1-Cl(Fe) and MUV-8-Cl(Fe) are quite robust, but not particularly thin (65 – 120 nm), limiting the conclusions that can be drawn about dimensionality effects on magnetic behaviour.

One of the biggest challenges for the exfoliation of layered MOFs lies in obtaining suitably sized single crystals to begin with. The weak bonding along the stacking direction of layered MOFs often leads to poor crystallinity, stacking faults and small crystallite sizes.[75–79] This, in turn, ultimately limits the quality and size of exfoliated material that can be obtained. Recently, a team based at Yale University have managed to overcome this challenge by employing the use of a functionalised anthracene dimer as a ligand (Fig. 7), forming a three-dimensional MOF which is capable of forming larger single crystals (~ 300 μm).[66] Subsequent thermal treatment breaks the dimerisation of the ligand, producing similarly sized single crystals of a layered MOF with pi-stacking interactions between the layers. The three-dimensional precursor MOF has the general formula, Zn_3BDC_3L, where BDC = 1,4-benzenedicarboxylic acid and *L* is a pyridyl-terminated dianthracene ligand, denoted $diAn^{CNC-3Py}$ (Fig. 8).

The novel synthesis pathway presented in Ref. 66 allows for selective functionalisation and direct incorporation of the dimer ligand into the three-dimensional MOF structure. This synthesis route produces large (~ 300 μm), colourless, plate-shaped single crystals. The structure consists of a secondary building unit (SBU) with three Zn^{2+} ions and six BDC molecules. Each SBU is linked by BDC molecules to form two-dimensional sheets and the terminal Zn ions in each SBU are connected to $diAn^{CNC-3Py}$ ligands in the stacking direction. Upon annealing at 210 °C, the ligand undimerises to form a two-dimensional MOF structure. π-stacking interactions between the anthracene on one layer, and the pyridine on an adjacent layer, hold the two-dimensional sheets together. These layers are then exfoliated using Scotch Magic™ tape and deposited onto a Si/SiO_2 substrate. The tape with exfoliated flakes was secured to the substrate surface and annealed at 100 °C for two minutes, before being allowed to cool for five minutes and peeled away.[66] The chemical composition of flakes was investigated using optical photothermal infrared spectroscopy (O-PTIR) and X-ray photoelectron spectroscopy (XPS). They confirm that the chemical composition seen in bulk is retained on exfoliation. In the supplementary information of Ref. 66, the authors also report data for a sample of 16 flakes,

View Article Online
DOI: 10.1039/D6CC02624A

including flake height, estimated area, mean roughness, and aspect ratio. In this way, we see that the thinnest flake obtained is 3.8 nm, which corresponds to a bilayer, but the average height across all sampled flakes is 15 nm.[66] The authors also show that flakes are typically quite large, with areas of up to 3500 nm^2. This detailed reporting of flake dimensions sets a precedent for future MOF exfoliation work, which we suggest should incorporate at least a qualitative description of the reproducibility of any exfoliation procedure, and ideally a statistical analysis of results, as presented here. Ref. 66 also demonstrates that single-crystal MOF growth is a key consideration in the engineering of novel layered MOFs suitable for exfoliation, and the new synthesis strategy presented in this work could be a route to achieving large, high-quality crystals and, therefore, improve the quality of nanosheets. Indeed, this work also opens the opportunity to utilise this novel synthesis strategy with alternative, paramagnetic metal, M^{2+}, ions, which may enable the discovery of new magnetic topologies in the two-dimensional limit.

Thus, in this section, through a comprehensive presentation of several key case studies, we have highlighted what we believe are the current key challenges associated with the Scotch tape exfoliation of magnetic MOFs. In summary, they are:

- Limited literature reporting of the Scotch tape exfoliation methodology, including full details of the procedure itself, tools used, deposition techniques and cleaning procedures.
- Limitations in crystal size and increased crystal fragility for MOFs, which is linked to their inter- and intra-plane interaction strengths. This is most likely the reason why MOF nanosheets are non-uniform in height, size and coverage and is a key factor in determining the sample thickness and quality achievable.
- Difficulty in applying surface-sensitive magnetic characterisation techniques to exfoliated MOFs.

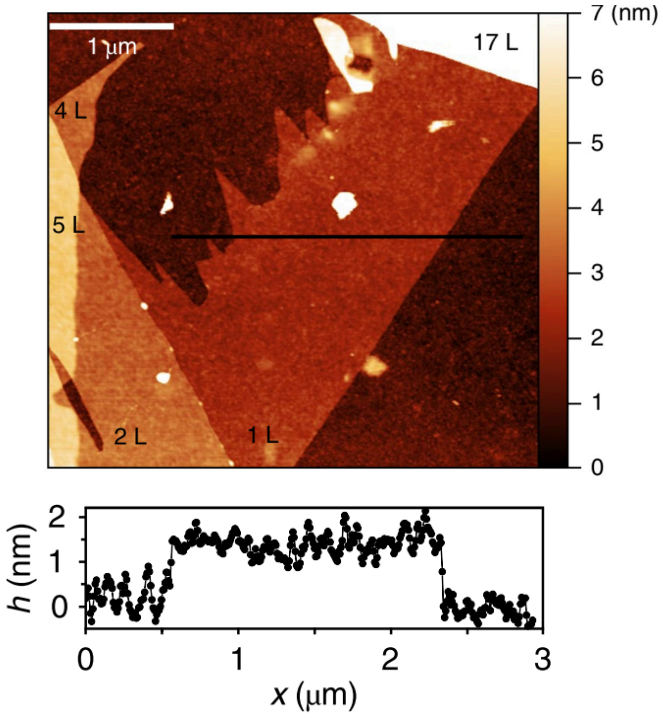

Fig. 5 AFM topographical image of a MUV-1-Cl(Fe) nanosheet obtained *via* Scotch tape exfoliation. The line profile indicates the monolayer section of the nanosheet (1L) which is ∼ 1.5 nm in height. Across the whole ∼ 4 x 4 μm AFM scan area, it can be seen that there are a variety of thicknesses within the one flake (2L = 2 layers, 4L = 4 layers, *etc*). Figure adapted from Ref. 50 with permission from Springer Nature,[50] copyright 2018.

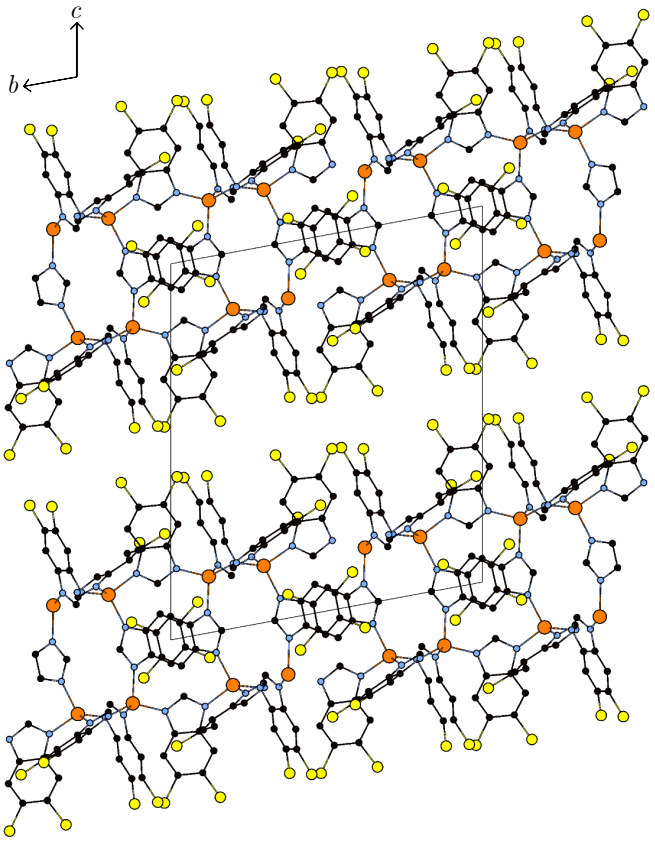

Fig. 6 Two Fe^{2+} "double-layers" of MUV-8-Cl(Fe) stacked in the *c*-axis direction. Fe^{2+} ions are coordinated to three $bimCl_2$ in the same plane, and a fourth in the *c*-axis direction to form this novel structure. Adjacent "double-layers" are held together in the *c*-axis direction by van der Waals interactions between the chlorine atoms. Fe, orange; C, black; N, light blue; Cl, yellow. Hydrogen atoms and disordered ferrocenes between the layers have been omitted for clarity.

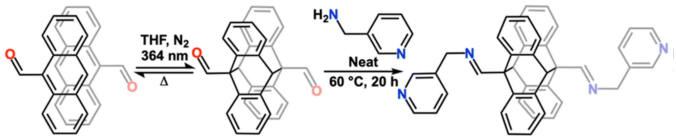

Fig. 7 Novel synthesis pathway developed by Logelin *et. al.* to synthesise the dimer ligand, $diAn^{CNC-3Py}$. Here they take the 9,9'-dianthraldehyde ligand and functionalise it with a primary amine to favour the pyridine-terminated dimer, $diAn^{CNC-3Py}$. Figure adapted from Ref. 66 with permission from the Royal Society of Chemistry,[66] copyright 2024.

View Article Online
DOI: 10.1039/D6CC02624A

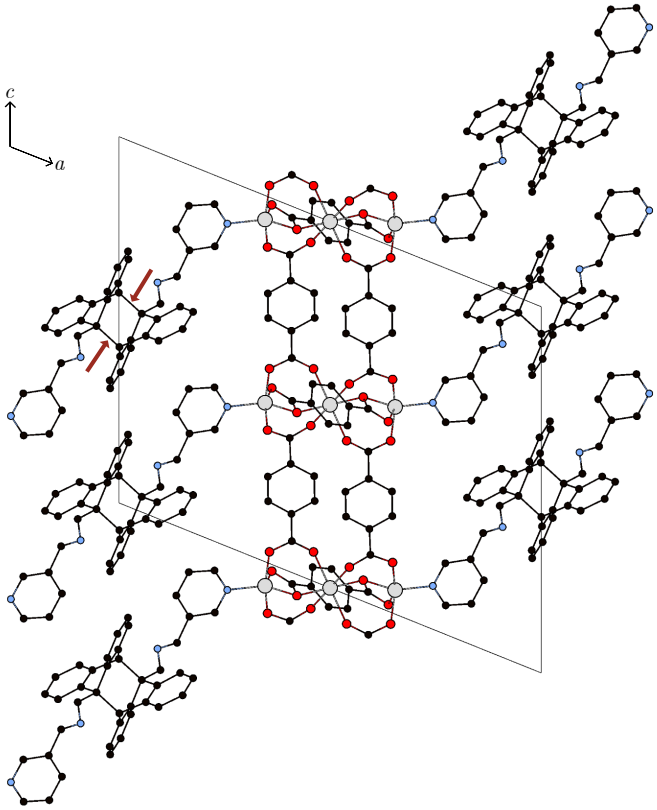

Fig. 8 Crystal structure of $Zn_3BDC_3(diAn^{CNC-3Py})$ shown along the *b*-axis direction. Three Zn atoms and six BDC molecules make up the SBU which are connected in the *c*-axis direction to form two-dimensional sheets. The terminal zinc ions in each SBU connect to $diAn^{CNC-3Py}$ ligands in the stacking direction (*a*-axis direction). When annealed at 210 °C, the dimer bonds, indicated here on one dimer with the red arrows, are cleaved. This results in the two-dimensional MOF with π-stacking interactions between an anthracene on one layer and a pyridine on the adjacent layer. Zn, grey; C, black; N, light blue; O, red. Hydrogen atoms and solvent molecules removed for clarity.

In the following section we will explore these challenges in more detail, and suggest the ways in which we believe they can be tackled by the wider research community.

Overcoming challenges and future directions

A community-wide effort to create and adhere to reporting protocols for exfoliation methods

The lack of rigorous reporting of Scotch tape exfoliation methodology is a fundamental shortcoming for the two-dimensional materials community, in general. This is exacerbated in the exploration of two-dimensional MOFs, where Scotch tape exfoliation is typically more difficult to achieve, and requires a more nuanced approach. Overcoming this barrier requires a concerted effort from the entire research community. Strategies could involve co-creating guidelines for the reporting of exfoliation methods, which could be implemented in peer review. As a general framework, we suggest reporting, at minimum, the following methodological information to (i) facilitate wider adoption of the technique across the community and (ii) enable researchers to assess the validity and reproducibility of research outcomes in the field:

- Substrate preparation procedures, including substrate cleaning pre- and post-deposition.
- Detailed description of the exfoliation procedure employed, including the type of tape used, number of exfoliation steps, and conditions under which the exfoliation was performed, *i.e.* ambient, glovebox *etc.*
- Deposition procedures, *e.g.* deposition temperature, details of any transfer steps or any substrate dependence.
- Representative optical and AFM images of exfoliated flakes, with any artefacts, *e.g.*, adhesive or atmospheric contamination, identified and explained.
- The range of nanosheet thicknesses and lateral dimensions achieved alongside an indication of how reproducibly these results were achieved. This could also include statistical analysis of such metrics across sampled flakes, as in, for example, Ref. 66.

Characterisation of MOF nanosheets by AFM is often particularly labour-intensive because of their small lateral dimensions and the low surface coverage typically achieved on substrates. In contrast, optical imaging is generally a more rapid and convenient technique and has therefore been used in the characterisation of two-dimensional inorganic materials, whose flakes are often substantially larger. For these materials, the thickness-dependent optical contrast of nanosheets has been exploited to generate optical calibration curves, allowing nanosheet thickness to be estimated directly from optical microscopy. Such calibration curves make the identification and selection of suitable nanosheets considerably faster and more reliable than relying on AFM alone.[80] There are also a number of ways in which flake identification has been automated for these materials.[81,82] Typically, these involve the use of machine learning (ML) algorithms for data segmentation. Similar techniques could be employed to exfoliated MOFs, but would first require the generation of sufficiently large and reliable training datasets. We argue that this can only be achieved through a community-wide effort, along the lines proposed above. We believe that clearer methodological reporting could transform the application of the Scotch tape method to MOFs by democratising the technique and facilitating the automated design and discovery of new two-dimensional materials.

Understanding the feasibility of Scotch tape exfoliation to different families of MOFs

The current state-of-the-art indicates that the feasibility and likely success of a Scotch tape exfoliation of a MOF, *i.e.*, whether it is possible to reproducibly obtain high-quality, sufficiently large and thin nanosheets, is highly sample-dependent. Whilst there are likely multiple underlying factors, we believe one of the main reasons stems from the challenges in growing suitably robust single crystals to facilitate Scotch tape exfoliation, in comparison to inorganic systems. The vast chemical space accessible to MOFs,

View Article Online
DOI: 10.1039/D6CC02624A

arising from their reticular design principles, means there are a huge range of intra-plane bonding motifs and intermolecular interactions that may govern the assembly of a layered MOF's structure. As a result, there will be enormous variety in the energy scales of their inter- and intra-plane interactions, which will directly affect the way in which they are exfoliated. Understanding this complex energy landscape may be central to elucidating the behaviour of layered MOFs upon exfoliation and, indeed, to predicting how successfully they may be exfoliated, not necessarily just by the Scotch tape method, but by other exfoliation methods as well. One way in which this may be achieved is through the use of density functional theory (DFT) calculations. Such methods have been applied to inorganic layered materials and are even capable of calculating the energy required to separate individual layers.[83,84] Of course, applying DFT to MOFs is challenging. They typically have a large number of atoms per unit cell, and often possess defects and disorder in their structures,[85] making calculations computationally expensive. Treating *layered, magnetic* MOFs with DFT is even more difficult. Dispersive interactions are typically not well treated by DFT and require additional corrections.[86–88] On top of this, describing two-dimensional magnetism with DFT also requires extra considerations.[89] Yet, progress *is* being made in addressing these challenges. For instance, DFT has been recently used to investigate magnetic van der Waals MOF structures.[48] Indeed, it is a powerful computational tool that could allow us to rationalise the exfoliation behaviour of layered MOFs and also predict their magnetic behaviour. Thus, further research effort to develop computational techniques for treating layered MOFs could prove extremely fruitful. Once exfoliation behaviour relative to MOF interactions is better understood, DFT- or ML-driven crystal structure prediction (CSP) could be used to engineer new two-dimensional MOF structures,[90] which possess the required characteristics to make them more amenable to exfoliation, and also incorporate motifs which could endow exotic magnetic behaviours.

As well as exploring ways to design new MOFs which are more amenable to exfoliation, we can also look to engineer new exfoliation tools which improve the exfoliation process. Indeed, this has recently been investigated for the inorganic TMDs, where Onodera *et al.* at the University of Tokyo have engineered a new adhesive tape for exfoliation.[91] They carry out a rigorous systematic study to show that, with this new tape, they are able to reproducibly achieve good coverage of high-quality monolayers and bilayers of WSe_2, which are up to ten times larger in lateral width than those obtained with the most commonly-used commercial tapes for TMDs.[91] Since TMDs are known to be more fragile than graphite, and thus are more susceptible to cracking on exfoliation,[71] this tape has been designed with optimised adhesive flatness and a rigid tape backing, which prevents flake wrinkling and cracking.[91] Since, as we have highlighted, the in-plane fragility of MOFs is one of the limiting factors to successful exfoliation, applying a tape such as this to MOF exfoliation may improve results. Furthermore, as a community we can work to optimise tape design specifically for MOFs, which when done in a systematic way such as this,[91] could prove highly advantageous.

Developing existing surface-sensitive magnetic characterisation techniques and exploring new ones

The final major challenge associated with exfoliated magnetic MOFs that we have highlighted in the view is the current lack of magnetic characterisation techniques that can be applied to them. The most common quantitative characterisation techniques applied to inorganic two-dimensional magnets, like MOKE or nitrogen vacancies (NV) magnetometry,[92] require micron-sized flakes of uniform thickness and, therefore, are unsuitable for MOFs where flakes, as we have seen, are typically smaller and non-uniform. In addition, these techniques can be destructive for MOFs, which are often fragile and sensitive to radiation.[93,94] X-ray magnetic circular dichroism (XMCD) or X-ray magnetic linear dichroism (XMLD) are synchrotron soft X-ray spectroscopy techniques which can be used to investigate ferromagnetism, or antiferromagnetism, in two-dimensional materials, respectively.[95,96] It is a highly surface-sensitive technique, which has been used in a number of cases to investigate the magnetic phase behaviour in the two-dimensional limit for inorganic materials.[97] Whilst exposure to synchrotron radiation has been known to damage MOFs,[94] this technique has the advantage of being quite tuneable, meaning beam intensity can be modulated to reduce sample exposure and damage, and measurement protocols can be adapted to avoid unnecessary beam exposure. Indeed, this approach has been successfully carried out in the case of two magnetic MOFs,[98,99] and warrants further development and application.

In summary, we suggest that advancing the field of exfoliated two-dimensional magnetic MOFs will require coordinated progress across experimental practice, data generation, sample characterisation, and theory. Standardised and transparent reporting of Scotch tape exfoliation methodologies would significantly improve reproducibility and enable the creation of large, reliable datasets that could support automated flake identification and machine-learning approaches. At the same time, a deeper theoretical understanding through improved DFT and data-driven modelling of the interplay between intra- and interlayer interactions in layered MOFs could enable the prediction and design of structures more amenable to exfoliation. Finally, continued development and adaptation of surface-sensitive magnetic characterisation techniques will be essential for probing the properties of increasingly small and fragile MOF nanosheets. Together, we hope that these directions present a useful roadmap for future research, with the potential to unlock the systematic discovery and investigation of new two-dimensional MOF materials and their emergent magnetic phenomena.

Author contributions

EJE and LC developed the concept for the review. EJE led the review of the literature and wrote the first draft. EJE and LC revised and finalised the manuscript.

Conflicts of interest

There are no conflicts to declare.

View Article Online
DOI: 10.1039/D6CC02624A

Data availabilty

Data sharing is not applicable to this article as no new datasets were generated or analysed during the current study.

Acknowledgements

The authors acknowledge the Engineering and Physical Sciences Research Council (EPSRC) Centre for Doctoral Training in Topological Design for the provision of a PhD studentship to EJE. This work was also supported by the EPSRC grant EP/T02271X/1.

Notes and references

1 K. S. Novoselov, A. K. Geim, S. V. Morozov, D. Jiang, Y. Zhang, S. V. Dubonos, I. V. Grigorieva and A. A. Firsov, *Science*, 2004, **306**, 666–669.
2 B. Radisavljevic, A. Radenovic, J. Brivio, V. Giacometti and A. Kis, *Nat. Nanotechnol.*, 2011, **6**, 147–150.
3 H. Li, G. Lu, Y. Wang, Z. Yin, C. Cong, Q. He, L. Wang, F. Ding, T. Yu and H. Zhang, *Small*, 2013, **9**, 1974–1981.
4 H. Li, J. Wu, Z. Yin and H. Zhang, *Acc. Chem. Res.*, 2014, **47**, 1067–1075.
5 D. Pacilé, J. C. Meyer, Girit and A. Zettl, *Appl. Phys. Lett.*, 2008, **92**, 133107.
6 E. Shi, S. Deng, B. Yuan, Y. Gao, Akriti, L. Yuan, C. S. Davis, D. Zemlyanov, Y. Yu, L. Huang and L. Dou, *ACS Nano*, 2019, **13**, 1635–1644.
7 D. Zhao, D. Gao, X. Wu, B. Li, S. Zhang, Z. Li, Q. Wang, Z. Wu, C. Zhang, W. C. Choy, X. Zhong, Q. He and Z. Zhu, *Adv. Mater.*, 2022, **34**, 2204661.
8 F. Ciccarelli, M. Barra, A. Carella, G. M. D. Luca, F. Gesuele and F. Chiarella, *Cryst.*, 2025, **15**, 1024.
9 K. S. Novoselov, D. Jiang, F. Schedin, T. J. Booth, V. V. Khotkevich, S. V. Morozov and A. K. Geim, *Procl. Natl. Acad. Sci. U. S. A.*, 2005, **102**, 10451–10453.
10 K. Matsuda, *J. Phys. Soc. Jpn.*, 2015, **84**, 121009.
11 A. Splendiani, L. Sun, Y. Zhang, T. Li, J. Kim, C. Y. Chim, G. Galli and F. Wang, *Nano Lett.*, 2010, **10**, 1271–1275.
12 K. F. Mak, C. Lee, J. Hone, J. Shan and T. F. Heinz, *Phys. Rev. Lett.*, 2010, **105**, 136805.
13 M. Chhowalla, H. S. Shin, G. Eda, L. J. Li, K. P. Loh and H. Zhang, *Nat. Chem.*, 2013, **5**, 263–275.
14 R. Moqbel, L.-T. Huang, K.-H. Lin, J. Bradford, K. Rahman, J. Felton, D. G. Papageorgiou, M. Dong, H. Zhang, M. Liu and R. J. Young, *2D Mater.*, 2024, **12**, 012002.
15 A. Falin, Q. Cai, E. J. Santos, D. Scullion, D. Qian, R. Zhang, Z. Yang, S. Huang, K. Watanabe, T. Taniguchi, M. R. Barnett, Y. Chen, R. S. Ruoff and L. H. Li, *Nat. Commun.*, 2017, **8**, 15815.
16 J. C. Blancon, H. Tsai, W. Nie, C. C. Stoumpos, L. Pedesseau, C. Katan, M. Kepenekian, C. M. Soe, K. Appavoo, M. Y. Sfeir, S. Tretiak, P. M. Ajayan, M. G. Kanatzidis, J. Even, J. J. Crochet and A. D. Mohite, *Science*, 2017, **355**, 1288–1292.
17 S. Chen, S. Wang, W. Xiong, al, Y. Hui, J. Lu, H. Jiang, D. S. Baji, A. V. Nair, S. Nair, S. Wei, X. Liao, C. Wang, J. Li, H. Zhang, Y.-J. Zeng, J. Linghu, H. Jin and Y. Wei, *2D Mater.*, 2020, **8**, 012005.
18 N.D. and H. M. Wagner, *Phys. Rev. Lett.*, 1966, **17**, 1133–1136.
19 K. De'Bell, A. MacIsaac and J. Whitehead, *Rev. Mod. Phys.*, 2000, **72**, 225.
20 L.-P. Regnault, *Encyclopedia of Materials: Science and Technology*, 2001, 856–864.
21 B. Zhang, P. Lu, R. Tabrizian, P. X. Feng and Y. Wu, *npj Spintron.*, 2024, **2**, 6–.
22 Z. Zhao, Y. Lin and A. Avsar, *npj 2D Mater. Appl.*, 2025, **9**, 30–.
23 M. Dabrowski, S. Guo, M. Strungaru, P. S. Keatley, F. Withers, E. J. Santos and R. J. Hicken, *Nat. Commun.*, 2022, **13**, 5976–.
24 B. Ilyas, T. Luo, A. von Hoegen, E. V. Boström, Z. Zhang, J. Park, J. Kim, J. G. Park, K. A. Nelson, A. Rubio and N. Gedik, *Nature*, 2024, **636**, 609–614.
25 B. Huang, G. Clark, E. Navarro-Moratalla, D. R. Klein, R. Cheng, K. L. Seyler, D. Zhong, E. Schmidgall, M. A. McGuire, D. H. Cobden, W. Yao, D. Xiao, P. Jarillo-Herrero and X. Xu, *Nature*, 2017, **546**, 270–273.
26 C. Gong, L. Li, Z. Li, H. Ji, A. Stern, Y. Xia, T. Cao, W. Bao, C. Wang, Y. Wang, Z. Q. Qiu, R. J. Cava, S. G. Louie, J. Xia and X. Zhang, *Nature*, 2017, **546**, 265–269.
27 J. M. Kosterlitz and D. J. Thouless, *J. Phys. C : Solid State Phys.*, 1973, **6**, 1181.
28 R. Roemer, C. Liu and K. Zou, *npj 2D Mater. Appl.*, 2020, **4**, 33–.
29 M. Bonilla, S. Kolekar, Y. Ma, H. C. Diaz, V. Kalappattil, R. Das, T. Eggers, H. R. Gutierrez, M. H. Phan and M. Batzill, *Nat. Nanotechnol.*, 2018, **13**, 289–293.
30 L. Hu, H. X. Wang, Y. Chen, K. Xu, M. R. Li, H. Liu, P. Gu, Y. Wang, M. Zhang, H. Yao and Q. Xiong, *Phys. Rev. B*, 2023, **107**, L220407.
31 L. Martín-Pérez, S. M. Rivero, M. V. Sulleiro, A. Naranjo, I. J. Gómez, M. L. Ruíz-González, A. Castellanos-Gomez, M. Garcia-Hernandez, E. M. Pérez and E. Burzurí, *ACS Nano*, 2023, **17**, 3007–3018.
32 T. Zhang, M. Grzeszczyk, J. Li, W. Yu, H. Xu, P. He, L. Yang, Z. Qiu, H. Lin, H. Yang, J. Zeng, T. Sun, Z. Li, J. Wu, M. Lin, K. P. Loh, C. Su, K. S. Novoselov, A. Carvalho, M. Koperski and J. Lu, *J. Am. Chem. Soc.*, 2022, **144**, 5295–5303.
33 D. Shcherbakov, P. Stepanov, D. Weber, Y. Wang, J. Hu, Y. Zhu, K. Watanabe, T. Taniguchi, Z. Mao, W. Windl, J. Goldberger, M. Bockrath and C. N. Lau, *Nano Lett.*, 2018, **18**, 4214–4219.
34 W. Pei, Z. Xiong, Y. Liu, X. Wu, Z. V. Han, S. Zhao, T. Zhang, W. Pei, Z. Xiong, Y. Liu, X. Wu, Z. V. Han, S. Zhao and T. Zhang, *Magnetochemistry*, 2023, **9**, 104.
35 W. Xie, J. Zhang, Y. Bai, Y. Liu, H. Wang, P. Yu, J. Li, H. Chang, Z. Wang, F. Gao, G. Wei, W. Zhao and T. Nie, *APL Mater.*, 2024, **12**, 031102.
36 W. Yu, J. Li, T. S. Herng, Z. Wang, X. Zhao, X. Chi, W. Fu, I. Abdelwahab, J. Zhou, J. Dan, Z. Chen, Z. Chen, Z. Li, J. Lu, S. J. Pennycook, Y. P. Feng, J. Ding and K. P. Loh, *Adv. Mater.*, 2019, **31**, 1903779.
37 M. Ramos, F. Carrascoso, R. Frisenda, P. Gant, S. Mañas-Valero, D. L. Esteras, J. J. Baldoví, E. Coronado,

View Article Online
DOI: 10.1039/D6CC02624A

A. Castellanos-Gomez and M. R. Calvo, *npj 2D Mater. Appl.*, 2021, **5**, 19–.

38 H. Lu, W. Wang, Y. Liu, L. Chen, Q. Xie, H. Yin, G. Cheng and L. He, *Appl. Surf. Sci.*, 2020, **504**, 144405.

39 D. Zhao, D. J. Timmons, D. Yuan and H. C. Zhou, *Acc. Chem. Res.*, 2010, **44**, 123–133.

40 A. E. Thorarinsdottir and T. D. Harris, *Chem. Rev.*, 2020, **120**, 8716–8789.

41 M. O'Keeffe, *Chem. Soc. Rev.*, 2009, **38**, 1215–1217.

42 V. R. Remya and M. Kurian, *Int. Nano Lett.*, 2018, **9**, 17–29.

43 X. Gao, X. Hai, H. Baigude, W. Guan and Z. Liu, *Sci. Rep.*, 2016, **6**, 37705–.

44 H. Li, K. Wang, Y. Sun, C. T. Lollar, J. Li and H. C. Zhou, *Mater. Today*, 2018, **21**, 108–121.

45 D. Li, A. Yadav, H. Zhou, K. Roy, P. Thanasekaran and C. Lee, *Global Challenges*, 2024, **8**, 2300244.

46 *Press release: Nobel Prize in Chemistry 2025*, `https://www.nobelprize.org/prizes/chemistry/2025/press-release/`.

47 J. Pitcairn, A. Iliceto, L. Cañadillas-Delgado, O. Fabelo, C. Liu, C. Balz, A. Weilhard, S. P. Argent, A. J. Morris and M. J. Cliffe, *J. Am. Chem. Soc.*, 2023, **145**, 1783–1792.

48 J. Pitcairn, M. A. Ongkiko, A. Iliceto, P. J. Speakman, S. Calder, M. J. Cochran, J. A. Paddison, C. Liu, S. P. Argent, A. J. Morris and M. J. Cliffe, *J. Am. Chem. Soc.*, 2024, **146**, 19146–19159.

49 D. J. Ashworth and J. A. Foster, *J. Mater. Chem. A*, 2018, **6**, 16292–16307.

50 J. López-Cabrelles, S. Mañas-Valero, I. J. Vitórica-Yrezábal, P. J. Bereciartua, J. A. Rodríguez-Velamazán, J. C. Waerenborgh, B. J. Vieira, D. Davidovikj, P. G. Steeneken, H. S. van der Zant, G. M. Espallargas and E. Coronado, *Nat. Chem.*, 2018, **10**, 1001–1007.

51 J. López-Cabrelles, S. Manas-Valero, In, J. Vitórica-Yrezábal, M. Lee, P. G. Steeneken, H. S. J. V. D. Zant, G. M. Espallargas and E. Coronado, *J. Am. Chem. Soc*, 2021, **143**, 18502–18510.

52 J. López-Cabrelles, S. Mañas-Valero, I. J. Vitórica-Yrezábal, P. J. Bereciartua, E. Coronado and G. M. Espallargas, *Dalton Trans.*, 2022, **51**, 1861.

53 R. B. Nielsen, K. O. Kongshaug and H. Fjellvåg, *J. Mater. Chem.*, 2008, **18**, 1002–1007.

54 H. L. Boström, S. Emmerling, F. Heck, C. Koschnick, A. J. Jones, M. J. Cliffe, R. A. Natour, M. Bonneau, V. Guillerm, O. Shekhah, M. Eddaoudi, J. Lopez-Cabrelles, S. Furukawa, M. Romero-Angel, C. Martí-Gastaldo, M. Yan, A. J. Morris, I. Romero-Muñiz, Y. Xiong, A. E. Platero-Prats, J. Roth, W. L. Queen, K. S. Mertin, D. E. Schier, N. R. Champness, H. H. Yeung and B. V. Lotsch, *Adv. Mater.*, 2024, **36**, 2304832.

55 J. C. Tan, P. J. Saines, E. G. Bithell and A. K. Cheetham, *ACS Nano*, 2012, **6**, 615–621.

56 H. Zhang, J. Huang, Y. Wang, R. Liu, X. Huai, J. Jiang and C. Anfuso, *Opt. Commun.*, 2018, **406**, 3–17.

57 D. J. Ashworth, A. Cooper, M. Trueman, R. W. M. Al-Saedi, L. D. Smith, A. J. H. M. Meijer and J. A. Foster, *Chem. - Eur. J.*, 2018, **24**, 17986–17996.

58 Y. Ding, Y. P. Chen, X. Zhang, L. Chen, Z. Dong, H. L. Jiang, H. Xu and H. C. Zhou, *J. Am. Chem. Soc.*, 2017, **139**, 9136–9139.

59 J. M. Moore and D. T. Genna, *Chem. - Eur. J.*, 2024, **30**, e202401713.

60 Y. Yang, A. Broto-Ribas, B. Ortín-Rubio, I. Imaz, F. Gándara, A. Carné-Sánchez, V. Guillerm, S. Jurado, F. Busqué, J. Juanhuix and D. Maspoch, *Angew. Chem. Int. Ed.*, 2022, **61**, e202111228.

61 P. Fernández-Seriñán, P. Samanta, I. Imaz and D. Maspoch, *J. Am. Chem. Soc*, 2025, **147**, 45849–45854.

62 Y. T. Guo and S. S. Yi, *Materials*, 2023, **16**, 5798.

63 H. U. Escobar-Hernandez, L. M. Pérez, P. Hu, F. A. Soto, M. I. Papadaki, H. C. Zhou and Q. Wang, *Ind. Eng. Chem. Res.*, 2022, **61**, 5853–5862.

64 K. Zhang, Z. B. Fang, Q. Q. Huang, A. A. Zhang, J. L. Li, J. Y. Li, Y. Zhang, T. Zhang and R. Cao, *Inorg. Chem.*, 2023, **62**, 8472–8477.

65 A. Abherve, S. Manas-Valero, M. Clemente-Leon and E. Coronado, *Chem. Sci.*, 2015, **6**, 4665–4673.

66 M. E. Logelin, E. Schreiber, B. Q. Mercado, M. J. Burke, C. M. Davis and A. K. Bartholomew, *Chem. Sci.*, 2024, **15**, 15198–15204.

67 Y. Wang, M. E. Ziebel, L. Sun, J. T. Gish, T. J. Pearson, X. Z. Lu, A. E. Thorarinsdottir, M. C. Hersam, J. R. Long, D. E. Freedman, J. M. Rondinelli, D. Puggioni and T. D. Harris, *Chem. Mater.*, 2021, **33**, 8712–8721.

68 H. Sun, Y. Yang, Y. Wang and L. Sun, *ACS Mater. Lett.*, 2026, **8**, 1413–1420.

69 A. Abherve, M. Abherve, C.-L. Leon, E. Coronado, C. J. Gomezgomez-García and M. Verneret, *Inorg. Chem.*, 2014, **53**, 12014–12026.

70 W. Wang, N. Clark, M. Hamer, A. Carl, E. Tovari, S. Sullivan-Allsop, E. Tillotson, Y. Gao, H. de Latour, F. Selles, J. Howarth, E. G. Castanon, M. Zhou, H. Bai, X. Li, A. Weston, K. Watanabe, T. Taniguchi, C. Mattevi, T. H. Bointon, P. V. Wiper, A. J. Strudwick, L. A. Ponomarenko, A. V. Kretinin, S. J. Haigh, A. Summerfield and R. Gorbachev, *Nat. Electron.*, 2023, **6**, 981–990.

71 L. J. Ji, Y. Qin, D. Gui, W. Li, Y. Li, X. Li and P. Lu, *Chem. Mater.*, 2018, **30**, 8732–8738.

72 S. Trejo, J. J. Antonio, E. Kraka and H. Chen, *J. Phys. Chem. C*, 2026, **130**, 2847–2854.

73 S. Jenkins, L. Rózsa, U. Atxitia, R. F. Evans, K. S. Novoselov and E. J. Santos, *Nat. Commun.*, 2022, **13**, 6917–.

74 M. Šiškins, M. Lee, S. Mañas-Valero, E. Coronado, Y. M. Blanter, H. S. van der Zant and P. G. Steeneken, *Nat. Commun.*, 2020, **11**, 2698–.

75 J. H. Dou, M. Q. Arguilla, Y. Luo, J. Li, W. Zhang, L. Sun, J. L. Mancuso, L. Yang, T. Chen, L. R. Parent, G. Skorupskii, N. J. Libretto, C. Sun, M. C. Yang, P. V. Dip, E. J. Brignole, J. T. Miller, J. Kong, C. H. Hendon, J. Sun and M. Dincă, *Nat. Mater.*, 2021, **20**, 222–228.

View Article Online
DOI: 10.1039/D6CC02624A

76 D. G. Ha, M. Rezaee, Y. Han, S. A. Siddiqui, R. W. Day, L. S. Xie, B. J. Modtland, D. A. Muller, J. Kong, P. Kim, M. Dincă and M. A. Baldo, *ACS Cent. Sci.*, 2020, **7**, 104–109.

77 M. Ko, L. Mendecki and K. A. Mirica, *Chem. Commun.*, 2018, **54**, 7873–7891.

78 E. M. Johnson, S. Ilic and A. J. Morris, *ACS Central Science*, 2021, **7**, 445–453.

79 Y. Lu, Y. Fu, Z. Hu, S. Feng, M. Torabi, L. Gao, S. Fu, Z. Wang, C. Huang, X. Huang, M. Wang, N. Israel, E. Dmitrieva, H. I. Wang, M. Bonn, P. Samorì, R. Dong, E. Coronado and X. Feng, *J. Am. Chem. Soc.*, 2025, **147**, 8778–8784.

80 H. Li, J. Wu, X. Huang, G. Lu, J. Yang, X. Lu, Q. Xiong and H. Zhang, *ACS Nano*, 2013, **7**, 10344–10353.

81 R. M. Sterbentz, K. L. Haley and J. O. Island, *Sci. Rep.*, 2021, **11**, 5808–.

82 P. A. Leger, A. Ramesh, T. Ulloa and Y. Wu, *Sci. Rep.*, 2024, **14**, 27808–.

83 J. H. Jung, C. H. Park and J. Ihm, *Nano Lett.*, 2018, **18**, 2759–2765.

84 M. Cutini, L. Maschio and P. Ugliengo, *J. Chem. Theory Comput.*, 2020, **16**, 5244–5252.

85 A. K. Cheetham, T. D. Bennett, F. X. Coudert and A. L. Goodwin, *Dalton Trans.*, 2016, **45**, 4113–4126.

86 S. Grimme, *J. Comput. Chem.*, 2006, **27**, 1787–1799.

87 E. R. Johnson, I. D. Mackie and G. A. DiLabio, *J. Phys. Org. Chem.*, 2009, **22**, 1127–1135.

88 S. Grimme, S. Ehrlich and L. Goerigk, *J. Comput. Chem.*, 2011, **32**, 1456–1465.

89 J. G. Aldea, D. L. Esteras, S. Roche and J. H. Garcia, *Nanoscale*, 2025, **17**, 24955–24989.

90 J. Park, H. Kim, Y. Kang, Y. Lim and J. Kim, *JACS Au*, 2024, **4**, 3727–3743.

91 M. Onodera, M. Ando, T. Hashimoto and T. Machida, *ACS Appl. Eng. Mater.*, 2026, **4**, 836–845.

92 L. Thiel, Z. Wang, M. A. Tschudin, D. Rohner, I. Gutiérrez-Lezama, N. Ubrig, M. Gibertini, E. Giannini, A. F. Morpurgo and P. Maletinsky, *Science*, 2019, **364**, 973–976.

93 X. Xu, L. Xia, C. Zheng, Y. Liu, D. Yu, J. Li, S. Zhong, C. Li, H. Song, Y. Liu, T. Sun, Y. Li, Y. Han, J. Zhao, Q. Lin, X. Li and Y. Zhu, *Nat. Commun.*, 2025, **16**, 261.

94 R. N. Widmer, G. I. Lampronti, N. Casati, S. Farsang, T. D. Bennett and S. A. Redfern, *Phys. Chem. Chem. Phys.*, 2019, **21**, 12389–12395.

95 G. van der Laan and A. I. Figueroa, *Coord. Chem. Rev.*, 2014, **277-278**, 95–129.

96 C. A. F. Vaz, G. V. D. Laan, S. A. Cavill, H. A. Dürr, A. F. Rodríguez, F. Kronast, W. Kuch, P. Sainctavit, G. Schütz, H. Wende, E. Weschke and . F. Wilhelm, *Nat. Rev. Methods Primers*, 2025, 27.

97 A. Bedoya-Pinto, J. R. Ji, A. K. Pandeya, P. Gargiani, M. Valvidares, P. Sessi, J. M. Taylor, F. Radu, K. Chang and S. S. Parkin, *Science*, 2021, **374**, 616–620.

98 S. Feng, H. Duan, H. Tan, F. Hu, C. Liu, Y. Wang, Z. Li, L. Cai, Y. Cao, C. Wang, Z. Qi, L. Song, X. Liu, Z. Sun and W. Yan, *Nat. Commun.*, 2023, **14**, 1–9.

99 J. Lobo-Checa, L. Hernández-López, M. M. Otrokov, I. Piquero-Zulaica, A. E. Candia, P. Gargiani, D. Serrate, F. Delgado, M. Valvidares, J. Cerdá, A. Arnau and F. Bartolomé, *Nat. Commun.*, 2024, **15**, 1–8.

View Article Online
DOI: 10.1039/D6CC02624A

Data availabilty

Data sharing is not applicable to this article as no new datasets were generated or analysed during the current study.